The structural flexibility of the shank1 PDZ domain is important for its binding to different ligands

Jun Hyuck Lee [a],[*],[1], HaJeung Park [b],[1], Soo Jeong Park [c], Hak Jun Kim [a], Soo Hyun Eom [c],[*]

[a] Korea Polar Research Institute, Incheon 406-840, South Korea
[b] Department of Cancer Biology, The Scripps Research Institute, Jupiter, FL 33458, USA
[c] Department of Life Science, Gwangju Institute of Science and Technology, Gwangju 500-712, South Korea

ARTICLE INFO

ABSTRACT

The PDZ domain of the shank protein interacts with numerous cell membrane receptors and cytosolic proteins via the loosely defined binding motif X-(Ser/Thr)-X-Φ-COOH (Φ represents hydrophobic residues) at the carboxyl terminus of its target protein. This enables shank to serve as a membrane-associated scaffold for the assembly of signaling complexes. As the list of proteins that bind to the shank PDZ domain grows, it is not immediately clear what structural element(s) mediate this domain's target specificity or the plasticity required to bind its different targets. Here, we have determined the crystal structure of the shank1 PDZ in complex with the βPIX C-terminal pentapeptide (642–646, DETNL) at 2.3 Å resolution and modeled shank1 PDZ binding to selected pentapeptide ligands. The resulting structures revealed a large hydrophobic pocket within the PDZ domain that can accommodate a variety of ligand residues at the P(0) position. A H-bond between His735 and Ser/Thr at the P(−2) position is invariant throughout the model structures. In addition, we identified multiple PDZ domain residues that are able to form H-bonds and salt bridges with an incoming target protein. Overall, our study provides a new level of understanding of the specificity and structural plasticity of the shank PDZ domain.

© 2011 Elsevier Inc. All rights reserved.

1. Introduction

Shank family proteins (shank1–3) are neuronal scaffold proteins that are involved in the formation of synaptic protein complexes. To carry out its functions, shank makes use of several protein interaction domains, including ankyrin repeats, an SH3 domain, a PDZ domain, a proline rich region and a SAM domain [1–3]. The PDZ (Postsynaptic density95/Discs large/Zona occludens-1) is a globular protein interaction domain of approximately 80–120 residues in length. Canonical PDZ domains contain six β-strands (βA–βF), a short α-helix (αA) and a long α-helix (αB) [19–21]. A groove created by αB and βB serves as the binding site for short peptide ligands. Shank PDZ domains interact with a variety of membrane proteins, including the calcium independent latrotoxin receptor [4,5], GluRδ2 [6], the Ca$_V$1.3 L-type voltage-gated calcium channel [7], mGluR5 [8], the receptor tyrosine kinase Ret9 [9], the cystic fibrosis transmembrane conductance regulator [10], Na$^+$/H$^+$ exchanger 3 [11], GluR1 [12], the somatostatin receptor type2 and the cytoplasmic proteins PLC-β3 [13], βPIX [14–16] and GKAP [2].

Although the shank PDZ domain recognizes the C-terminus of numerous target proteins, it is not yet clear how it achieves its target specificity or structural plasticity. Previous structural studies of the apo shank PDZ (PDB ID: 1Q3O) and the shank PDZ in complex with a GKAP C-terminal peptide (EAQTRL) (PDB ID: 1Q3P) showed a typical class I PDZ–ligand interaction with additional recognition sites at the P(−1), P(−3) and P(−5) positions of the ligand. The structure also revealed a novel PDZ–PDZ dimerization mechanism [17–26].

βPIX is a guanine nucleotide exchange factor for the small GTPases Rac1 and Cdc42, and contains several protein modules (SH3, Dlb homology, PH and leucine zipper domains) that can contribute to protein–protein and protein–lipid interactions [27–29]. βPIX plays an important role in the regulation of spine dynamics through its high-affinity binding to the shank PDZ via its carboxyl terminal motif (DETNL) [15,16].

In earlier studies, we showed that the shank PDZ asymmetrically binds to a βPIX trimer with a 1:3 stoichiometry and confirmed that the PDZ interaction sites on βPIX are concentrated at its C-terminal five amino acids [16]. In the present study, we aimed

to investigate the ligand binding specificity of the shank1 PDZ through elucidation of its structure at high-resolution. To that end, we solved the crystal structure of the PDZ domain in complex with the C-terminal pentapeptide of βPIX (DETNL) at a 2.3 Å resolution. We then modeled the binding of selected targets to this high resolution structure in an effort to better understand the binding plasticity of the PDZ domain. A comparison of our shank1 PDZ/βPIX complex and the shank1 PDZ/GKAP complex revealed the presence of both conserved and variable binding mechanisms. Furthermore, by combining structural and modeling analyses, we obtained new insight into how the structural plasticity of the shank PDZ enables recognition of multiple ligands.

2. Materials and methods

2.1. Protein expression and purification

The recombinant shank1 PDZ domain (residues 656–763) from *Rattus norvegicus* with a cleavable glutathione *S*-transferase (GST) tag was expressed in *Escherichia coli* BL21(DE3) and purified as previously described [30].

2.2. Crystallization and data collection for the shank1 PDZ:βPIX C-terminal peptide complex

The pentapeptide DETNL, which has the same amino acid sequence as the βPIX C-terminus, was synthesized by Anygen Co. (Korea). The Shank1 PDZ:βPIX complex was then prepared by mixing 10 mg/ml of the protein with the peptide stock at a 1:3 M ratio. Crystals of the shank1 PDZ:βPIX complex were grown by vapor diffusion using 1 μl of ∼0.8 mM complex and an equal volume of reservoir solution containing 100 mM sodium acetate (pH 5.5–6.0), 0.8 M lithium sulfate and 0.7 M ammonium sulfate at 21 °C. Successful flash freezing was achieved using Paratone-N oil (Hampton Research). A diffraction dataset with Bragg spacings of 2.3 Å was collected at beam line NW-AR12 at the Photon Factory (Tsukuba, Japan) using the X-ray beam at a single wavelength (1.000 Å). The data set was indexed and processed using the program HKL2000 (Table 1) [31]. Although the diffraction intensity of the spots were very strong at a 2.3 Å resolution, rejections due to over-

lapping spots caused data completeness to be relatively low in the highest resolution shell (83.7%).

2.3. Molecular replacement and structure refinement

The structure of the shank1 PDZ:βPIX complex was determined through molecular replacement using the program MOLREP [32]. For the cross-rotation search, the structure of the apo shank1 PDZ dimer (PDB code: 1Q3O) was used as the search model, and the highest peak of the rotation function (peak height: 9.8σ) was used for the translation function. This model gave a strong single peak in the translation function. An interpretable electron density map was calculated after rigid body refinement, simulated annealing; overall isotropic *B*-factor and individual restrained *B*-factor refinement were performed using the program CNS [33]. Iterative cycles of manual rebuilding using the program Coot [34] and subsequent refinement using CNS yielded a model with a final crystallographic *R* value of 23.5% (R_{free} = 26.7%) (Table 1). The atomic coordinates were deposited at the Protein Data Bank under accession code 3QJM.

2.4. Ligand modeling and energy minimization

Sequences of shank protein orthologs were obtained from the Uniprot server (www.uniprot.org) and aligned using ClustalX [35]. Selected pentapeptide ligands were modeled into the shank1-PDZ:βPIX complex by manually mutating the residues of βPIX in the program Coot [34]. The disordered residues (682–686) in the structure were modeled using the structure prediction tool in Prime 2.2 (Schrodinger, LLC, NY). The model structures were further idealized with allowances for C_α and side chain movements within 3 Å and 7.5 Å, respectively. The resulting coordinates were then energy-minimized with NAMD 2.7 [36] using the default settings of AutoIMD in VMD 1.8.7 [37].

3. Results and discussion

3.1. Overall structure of the shank1 PDZ–βPIX C-terminal peptide complex

The crystal structure of the shank1 PDZ–βPIX C-terminal peptide complex was solved by molecular replacement and refined to a 2.3 Å resolution with R_{cryst} = 23.5% and R_{free} = 26.7% (Fig. 1A). The Ramachandran plot calculated with the program PROCHECK [38] showed no residues with angular values in disallowed areas. The crystal belongs to the $P4_12_12$ space group with two shank1 PDZ–βPIX complexes per asymmetric unit. The final model included 207 amino acids and 56 water molecules (Fig. 1B). The structure was well-ordered with an average *B*-factor of 26.0 Å^2, except for the variable βA-βC loops in both chains (residues 682–686), which were disordered and thus not visible in the electron density map (Fig. 1C). Data collection and refinement statistics are summarized in Table 1. The structure of the shank1 PDZ–βPIX C-terminal peptide complex was also determined in orthorhombic space group (Table S1).

We found that the overall structure of the shank1 PDZ–βPIX complex is similar to the previously determined structure of the shank1 PDZ complexed with a GKAP C-terminal peptide (EAQTRL) [21]. The root mean square deviation (RMSD) between the two structures for 103 C_α positions was 0.69 Å. The shank PDZ monomer is composed of five β-strands (βA–βE) and two α-helices (αA and αB), with the peptide-binding site situated in a pocket between αB and βB. The shank1 PDZ exhibited a dimeric structure through its non-crystallographic two-fold symmetry (Fig. 1B),

Table 1
Data collection and refinement statistics.

Data set	
X-ray source	NW-AR12 beam line
Space group	$P4_12_12$
Wavelength (Å)	1.0000
Resolution (Å)	30–2.3 (2.38–2.3)
No. of measured reflections	45885
No. of unique reflections	10106
R_{sym}[a] (%)	3.2 (5.1)
Average I/σ	68.9 (36.4)
Data coverage total/final shell (%)	89.5/83.7
Redundancy	4.5
Refinement	
Resolution (Å)	25–2.3 (2.54–2.31)
No. of residues	207 (dimer)
No. of water molecules	56
R_{cryst}[b] total (%)	23.5 (22.5)
R_{free}[c] total (%)	26.7 (29.3)
R.M.S. bond length (Å)	0.008
R.M.S. bond angle (°)	1.135
Average B value (Å^2)	26.0

[a] $R_{sym} = \sum |\langle I \rangle - I| / \sum \langle I \rangle$.
[b] $R_{cryst} = \sum ||F_o| - |F_c|| / \sum |F_o|$.
[c] R_{free} calculated with 10% of all reflections excluded from refinement stages using high resolution data. Values in parentheses refer to the highest resolution shells.
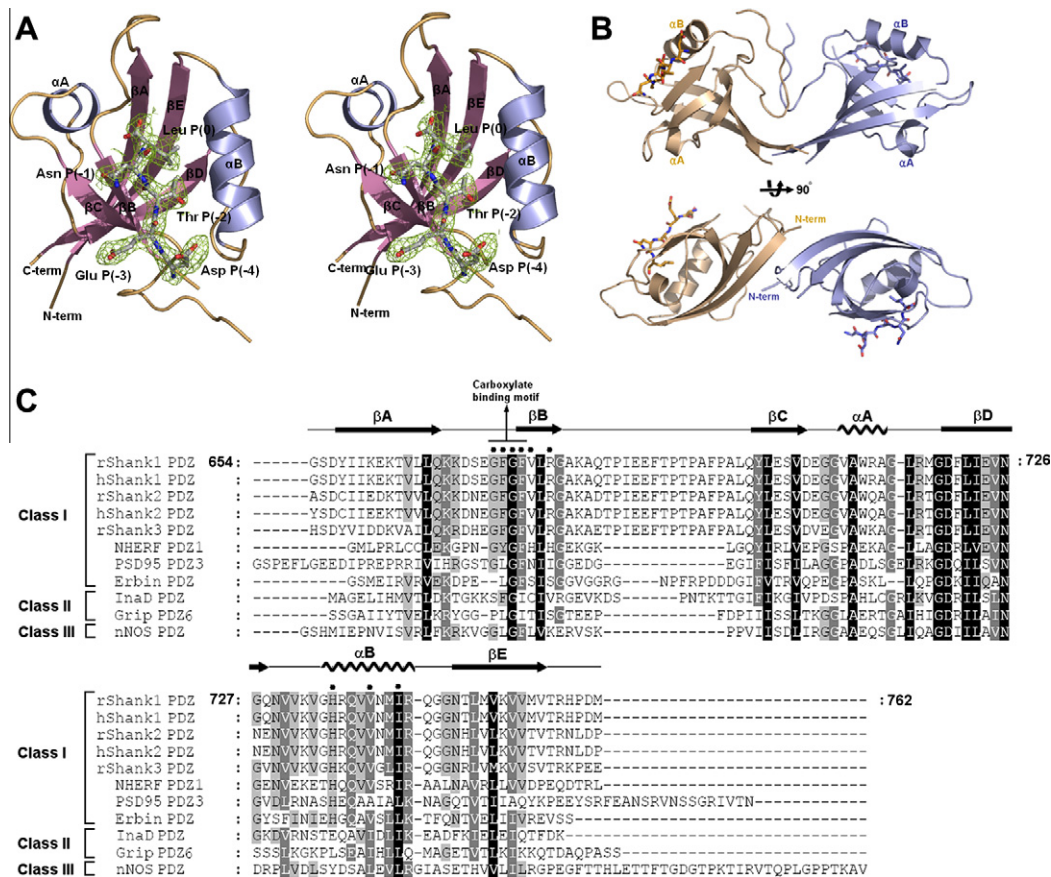
Fig. 1. Crystal structure of the shank1 PDZ in complex with the βPIX C-terminal peptide. (A) Stereoview of a ribbon diagram of the shank1 PDZ domain complexed with a βPIX C-terminal pentapeptide. The α-helices are labeled αA and αB; the β-strands are labeled βA through βE. Also shown is a 2Fo-Fc electron density map (contoured at 1σ) in which the bound βPIX C-terminal pentapeptide (DETNL) interacts with the shank1 PDZ domain. (B) Overall structure of the shank1 PDZ dimer. Each protomer is colored orange or blue. The bound peptide is shown as a stick model. (C) Sequence comparison of shank PDZ domains (rShank: *Rattus norvegicus* shank, hShank: human shank) and other PDZ domain proteins (PDB codes: NHERF PDZ1, 1I92; PSD95 PDZ3, 1BE9; Erbin PDZ, 1MFG/1MFL; InaD PDZ, 1IHJ; GRIP PDZ6, 1N7E/1N7F; nNOS PDZ, 1B8Q) [35]. Secondary structural elements and the carboxylate binding motif (with the leucine residue in the GLGF motif replaced by a phenylalanine) are indicated. The residues that constitute the core ligand-binding site are indicated by filled circles. (For interpretation of the references to colour in this figure legend, the reader is referred to the web version of this article.)

consistent with notion that PDZ homodimerization leads to shank self-association in solution [21].

3.2. Structural basis for the specificity of the shank PDZ–βPIX interaction

The βPIX C-terminal pentapeptide ligand bound as an additional strand to the anti-parallel β-sheet of the Shank1 PDZ, where it made extensive contacts with αB and βB. In the following discussion, the βPIX peptide C-terminal leucine residue will be referred to as Leu (0), and the remaining peptide residues will be numbered in descending order as Asn (−1), Thr (−2), Glu (−3) and Asp (−4). It was considered that three positions, P(0), P(−1) and P(−2), were the key determinants of target recognition by the PDZ. However, there is now evidence that residues upstream of the C-terminal tripeptide of the target may also be involved in the recognition process [19,22–24]. Both Leu (0) and Thr (−2) of the βPIX pentapeptide interact with the shank1 PDZ, consistent with the canonical class I mode of interaction that is exemplified by the structure of the shank1 PDZ–GKAP C-terminal peptide complex [21]. The carboxylate-binding loop, reflecting the two hydrogen (H−) bonds interactions between the terminal carboxyl group of Leu (0) and two main chain amide nitrogen atoms of Phe674 and Gly675, is also conserved. In addition, the Leu (0) side chain is inserted into a hydrophobic pocket formed by Phe674, Phe676, Leu678, Val739 and Ile742, and is partially covered by the aliphatic

part of Arg743. These modes of interaction are similar to those observed previously in the crystal structure of the shank PDZ in complex with the βPIX coiled-coil domain [16], except that the side chain rotation of Asn (−1) suggests that the P(−1) position is not critical for this interaction.
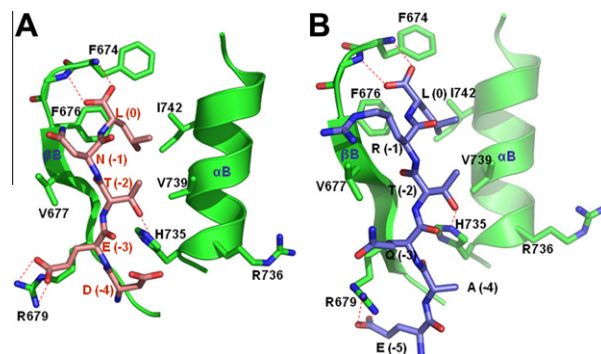

Fig. 2. Structural comparison of the shank1 PDZ–βPIX C-terminal peptide complex and the shank1 PDZ–GKAP C-terminal peptide complex. (A) Interaction mode of the βPIX C-terminal pentapeptide (DETNL: salmon) with the shank1 PDZ domain (green). (B) Interaction mode of the GKAP C-terminal pentapeptide (EAQTRL, slate blue) with the shank1 PDZ domain (green). The figures were made using PyMOL [40]. (For interpretation of the references to colour in this figure legend, the reader is referred to the web version of this article.)

Important differences between the shank1 PDZ bound to the βPIX pentapeptide or to the GKAP terminal peptide are found at Arg679 and Asp709 of the PDZ, which interact with P(−1), P(−3) and P(−5) of the ligand peptide. Arg679 is in the βB strand of the shank1 PDZ and makes a salt bridge with Glu (−3) of βPIX or Glu (−5) of GKAP. In addition, Asp709 forms a salt bridge with Arg (−1) of GKAP (for clarity, Asp709 is not shown in the same orientation in Fig. 2A and B). Whereas considerable variability was observed at the P(−1) position (Table 2), the residue at the P(0) position is strictly conserved. Likewise, the Thr residue at P(−2) is conserved and directly interacts with His735 in an αB helix within both complexes through the formation of a H-bond (Fig. 2).

3.3. Modeling and detailed binding mode analysis of pentapeptide ligands

The number of target proteins shown to bind to the shank PDZ is growing rapidly (Table 2). These proteins have different C-terminal sequences, suggesting that there may be means of target recognition other than those discussed above. To further characterize the binding pocket of the shank PDZ, we modeled select pentapeptides that have been reported to bind shank orthologs using the structure determined in the present work (Table 2). Sequence alignment of the orthologs showed that the peptide binding pockets are absolutely conserved among the species tested (Supplemental Fig. 1). We therefore carried out the ligand modeling

Table 2
Known shank PDZ interacting proteins and their C-terminal sequences.

Protein name		C-terminal sequence	Interacting partner	Reference
Membrane proteins	Human latrophilin/CIRL2/CL2	QLV**TSL**	Human shank1 PDZ	[4]
	Rat latrophilin/CIRL1/CL1	QLV**TSL**	Rat shank1/2/3 PDZ	[5]
	Ca$_V$1.3 L-type calcium channel	[b]MI**CITTL**	Rat shank1/3 PDZ	[7]
	mGluR5	QSS**SSL**	Rat shank1 PDZ	[8]
	Receptor tyrosine kinase Ret9	[b]HA**FTRF**	Rat shank3 PDZ	[9]
	Somatostatin receptor type 2	[b]DL**QTSI**	Rat shank2 PDZ human shank1 PDZ	[1]
	Cystic fibrosis transmembrane conductance regulator (CFTR)	VQD**TRL**	Rat shank2 PDZ	[10]
	Na$^+$/H$^+$ exchanger 3 (NHE3)	[b]PE**STHM**	Rat shank2 PDZ	[11]
	GluR1	LGA**TGL**	Mouse shank3 PDZ	[12]
	[a]GluRδ2	GluRδ2 internal sequence (893–921)	Rat shank1/2 PDZ	[6]
Cytosolic proteins	PLC-β3	EEN**TQL**	Rat shank2 PDZ	[13]
	β-PIX	[c]WDE**TNL**	Rat shank1/2/3 PDZ	[14,15]
	GKAP	[c]EAQ**TRL**	Rat shank1 PDZ	[2,21]

[a] The shank PDZ domain also binds directly to the internal sequence of the GluRδ2 protein.
[b] Structural modeling was done with the underlined sequence.
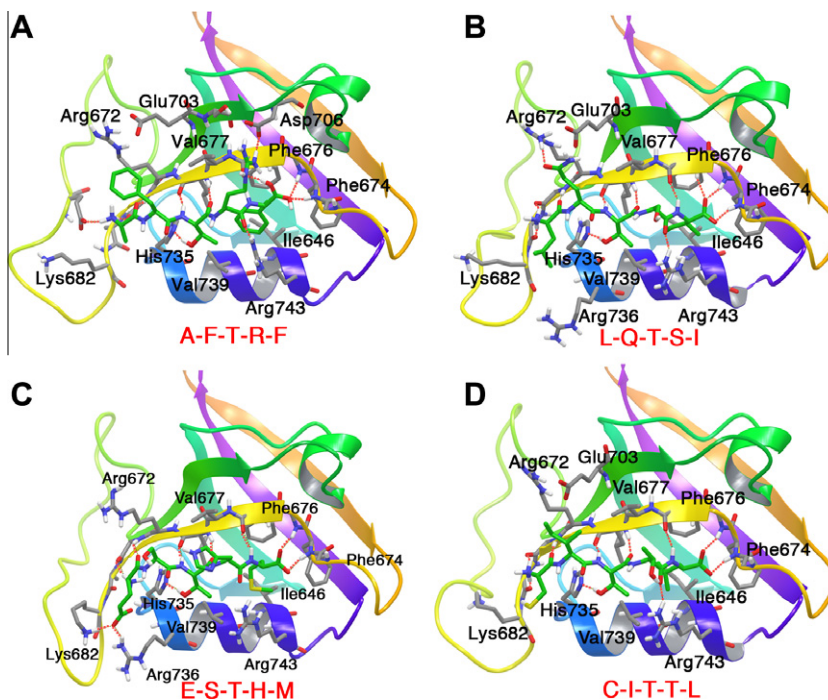[c] Crystal structure has been determined with this sequence.

Fig. 3. Comparison of shank1 PDZ–interacting peptides and switch residues in a shank1 PDZ–peptide complex model. Interaction mode of the receptor tyrosine kinase Ret9 C-terminal pentapeptide (AFTRF) (A), the somatostatin receptor type 2 C-terminal pentapeptide (LQTSI) (B), the Na$^+$/H$^+$ exchanger 3 C-terminal pentapeptide (ESTHM) (C), and the Ca$_V$1.3 L-type calcium channel C-terminal pentapeptide (CITTL) (D) with the rat shank1 PDZ. The bound peptides and the key PDZ residues involved in the interactions are shown in stick models. The PDZ domains are drawn as ribbon diagrams. H-bonds are represented as red dotted lines. The amino acid sequences of the bound peptides are written in red. (For interpretation of the references to colour in this figure legend, the reader is referred to the web version of this article.)

using the rat shank1 structure (this work) without editing any residues. The model structures showed that all side chains at the P(0) position point toward the hydrophobic pocket (Fig. 3). Surprisingly, it was apparent from the models that the hydrophobic pocket has ample space for a Phe or Met residue. We therefore modeled Trp in place of Phe, and found that the pocket is big enough to accommodate the indole ring of Trp. Though there is no known ligand that harbors a Trp at this position, this showed that the large hydrophobic pocket can easily accommodate side chains of various length and shape. In all of the model structures, the aliphatic part of Arg743 partially covered the hydrophobic pocket, and the guanidine group formed a salt bridge with the main chain carboxyl group of the residue at P(−1) (Fig. 3 and Supplemental Fig. 2).

The models differ from our observations in that the residues at the P(−1) position had little effect on PDZ binding. However, Asp706 is located close enough to the ligand to make a salt bridge when Arg is at P(−1), which is consistent with the crystal structure of the shank1 PDZ–GKAP complex (Fig. 3A and Supplemental Fig. 2A). The residue at the P(−2) position was always Ser or Thr, ensuring a H-bond with His735, which was invariant among the model structures. It has been suggested that the preference for a Thr residue at P(−2) reflects the hydrophobic interaction between the methyl group of Thr and Val739, the fifth residue (Val739 in shank PDZ) in the αB helix [20]. The residues at P(−3) and P(4) of the orthologs were mixed. Four residues (Glu, Gln, Asp or Asn) at these positions can potentially make H-bonds with Arg672 and Glu703 at P(−3) and Arg736 at P(−4) (Fig. 3B and C and Supplemental Fig. 2B and C). Ile or Phe at P(−3) appears to be marginally favorable, as one side of these residues makes a hydrophobic interaction with the aliphatic part of Arg672, while the other is exposed to the solvent. On the other hand, small hydrophobic residues, such as Leu and Ala, appear to be favored at P(−4) due to the presence of Arg and Lys, whose aliphatic side chains create a hydrophobic environment (Figs. 3A, B, and D and Supplemental Fig. 2A, B and D).

Overall, the structural plasticity of the shank PDZ arises from the characteristics of its binding surface, which includes a large hydrophobic pocket that can accommodate different sized side chains at P(0), the availability of multiple H-bonding partners for incoming peptides at P(−3) and P(−4), and a hydrophobic environment for small hydrophobic residues. The P(1) position has little impact on binding, though Asp706 can create an H-bond with the ligand when P(−1) is Arg. The invariant P(2) position is probably an anchor residue that registers the incoming peptide by making an H-bond with His735. These observations explain how one binding site in the shank PDZ can recognize multiple target proteins. There is also precedent for the suggestion that a single PDZ can bind multiple ligands through different modes of interaction. For example, the PDZ2 domain of syntenin interacts exclusively with the C-terminal peptide of the IL-5 receptor α-subunit (ETLEDSVF) and syndecan (TNEFYA), but the binding mode for each of these ligands is distinct (typical class I for the IL-5 receptor and class II for syndecan) [26]. Another example is the Par-6 PDZ domain, which binds both the C-terminal peptide (VKESLV) and an internal sequence of Pals1 (YPKHREMAVDCP) [39]. This implies that reconfiguration of the binding pocket to accommodate different ligands is not unique to the shank PDZ, but is a general feature of PDZ domains.

Acknowledgments

Appendix A. Supplementary data

References

[1] H. Zitzer, H.H. Honck, D. Bachner, D. Richter, H.J. Kreienkamp, Somatostatin receptor interacting protein defines a novel family of multidomain proteins present in human and rodent brain, J. Biol. Chem. 274 (1999) 32997–33001.

[2] S. Naisbitt, E. Kim, J.C. Tu, B. Xiao, C. Sala, J. Valtschanoff, R.J. Weinberg, P.F. Worley, M. Sheng, Shank a novel family of postsynaptic density proteins that binds to the NMDAreceptor/PSD-95/GKAP complex and cortactin, Neuron 23 (1999) 569–582.

[3] M. Sheng, E. Kim, The shank family of scaffold proteins, J. Cell Sci. 113 (2000) 1851–1856.

[4] H.J. Kreienkamp, H. Zitzer, E.D. Gundelfinger, D. Richter, T.M. Bockers, The calcium-independent receptor for alpha-latrotoxin from human and rodentbrains interacts with members of the ProSAP/SSTRIP/shank family of multidomainproteins, J. Biol. Chem. 275 (2000) 32387–32390.

[5] S. Tobaben, T.C. Sudhof, B. Stahl, The G protein-coupled receptor CL1 interacts directly with proteins of the shank family, J. Biol. Chem. 275 (2000) 36204–36210.

[6] T. Uemura, H. Mori, M. Mishina, Direct interaction of GluRdelta2 with shank scaffold proteins in cerebellar Purkinje cells, Mol. Cell. Neurosci. 26 (2004) 330–341.

[7] H. Zhang, A. Maximov, Y. Fu, F. Xu, T.S. Tang, T. Tkatch, D.J. Surmeier, I. Bezprozvanny, Association of CaV13 L-type calcium channels with shank, J. Neurosci. 25 (2005) 1037–1049.

[8] J.C. Tu, B. Xiao, S. Naisbitt, J.P. Yuan, R.S. Petralia, P. Brakeman, A. Doan, V.K. Aakalu, A.A. Lanahan, M. Sheng, P.F. Worley, Coupling of mGluR/Homer and PSD-95 complexes by the shank family of postsynaptic density proteins, Neuron 23 (1999) 583–592.

[9] G. Schuetz, M. Rosario, J. Grimm, T.M. Boeckers, E.D. Gundelfinger, W. Birchmeier, The neuronal scaffold protein shank3 mediates signaling and biological function of the receptor tyrosine kinase Ret in epithelial cells, J. Cell Biol. 167 (2004) 945–952.

[10] J.Y. Kim, W. Han, W. Namkung, J.H. Lee, K.H. Kim, H. Shin, E. Kim, M.G. Lee, Inhibitory regulation of cystic fibrosis transmembrane conductance regulator anion-transporting activities by shank2, J. Biol. Chem. 279 (2004) 10389–10396.

[11] W. Han, K.H. Kim, M.J. Jo, J.H. Lee, J. Yang, R.B. Doctor, O.W. Moe, J. Lee, E. Kim, M.G. Lee, Shank2 associates with and regulates Na+/H+ exchanger 3, J. Biol. Chem. 281 (2006) 1461–1469.

[12] S. Uchino, H. Wada, S. Honda, Y. Nakamura, Y. Ondo, T. Uchiyama, M. Tsutsumi, E. Suzuki, T. Hirasawa, S. Kohsaka, Direct interaction of post-synaptic density-95/Dlg/ZO-1 domain-containing synaptic molecule shank3 with GluR1 alpha-amino-3-hydroxy-5-methyl-4-isoxazole propionic acid receptor, J. Neurochem. 97 (2006) 1203–1214.

[13] J.I. Hwang, H.S. Kim, J.R. Lee, E. Kim, S.H. Ryu, P.G. Suh, The interaction of phospholipase C-beta3 with shank2 regulates mGluR-mediated calcium signal, J. Biol. Chem. 280 (2005) 12467–12473.

[14] S. Kim, S.H. Lee, D. Park, Leucine zipper-mediated homodimerization of the p21-activated kinase-interacting factor, beta Pix. Implication for a role in cytoskeletal reorganization, J. Biol. Chem. 276 (2001) 10581–10584.

[15] E. Park, M. Na, J. Choi, S. Kim, J.R. Lee, J. Yoon, D. Park, M. Sheng, E. Kim, The shank family of postsynaptic density proteins interacts with and promotes synaptic accumulation of the beta PIX guanine nucleotide exchange factor for Rac1 and Cdc42, J. Biol. Chem. 278 (2003) 19220–19229.

[16] Y.J. Im, G.B. Kang, J.H. Lee, K.R. Park, H.E. Song, E. Kim, W.K. Song, D. Park, S.H. Eom, Structural basis for asymmetric association of the betaPIX coiled coil and shank PDZ, J. Mol. Biol. 397 (2010) 457–466.

[17] B.Z. Harris, W.A. Lim, Mechanism and role of PDZ domains in signaling complex assembly, J. Cell Sci. 114 (2001) 3219–3231.

[18] A.Y. Hung, M. Sheng, PDZ domains: structural modules for protein complex assembly, J. Biol. Chem. 277 (2002) 5699–5702.

[19] G. Birrane, J. Chung, J.A. Ladias, Novel mode of ligand recognition by the Erbin PDZ domain, J. Biol. Chem. 278 (2003) 1399–1402.

[20] H.J. Lee, J.J. Zheng, PDZ domains and their binding partners: structure, specificity, and modification 8 (2010) 8.

[21] Y.J. Im, J.H. Lee, S.H. Park, S.J. Park, S-H. Rho, G.B. Kang, E. Kim, S.H. Eom, Crystal structure of the shank PDZ–ligand complex reveals a class I PDZ interaction and a novel PDZ–PDZ dimerization, J. Biol. Chem. 278 (2003) 48099–48104.

[22] T. Walma, C.A. Spronk, M. Tessari, J. Aelen, J. Schepens, W. Hendriks, G.W. Vuister, Structure dynamics and binding characteristics of the second PDZ domain of PTP-BL, J. Mol. Biol. 316 (2002) 1101–1110.

[23] G. Kozlov, D. Banville, K. Gehring, I. Ekiel, Solution structure of the PDZ2 domain from cytosolic human phosphatase hPTP1E complexed with a peptide reveals contribution of the beta2-beta3 loop to PDZ domain–ligand interactions, J. Mol. Biol. 320 (2002) 813–820.

[24] A. Piserchio, M. Pellegrini, S. Mehta, S.M. Blackman, E.P. Garcia, J. Marshall, D.F. Mierke, The PDZ1 domain of SAP90. Characterization of structure and binding, J. Biol. Chem. 277 (2002) 6967–6973.

[25] Y.J. Im, S.H. Park, S.-H. Rho, J.H. Lee, G.B. Kang, M. Sheng, E. Kim, S.H. Eom, Crystal structure of GRIP1 PDZ6–peptide complex reveals the structural basis for class II PDZ target recognition and PDZ domain-mediated multimerization, J. Biol. Chem. 278 (2003) 8501–8507.

[26] B.S. Kang, D.R. Cooper, Y. Devedjiev, U. Derewenda, Z.S. Derewenda, Molecular roots of degenerate specificity in syntenin's PDZ2 doma reassessment of the PDZ recognition paradigm, Structure 11 (2003) 845–853.

[27] E. Manser, T.H. Loo, C.G. Koh, Z.S. Zhao, X.Q. Chen, L. Tan, I. Tan, T. Leung, L. Lim, PAK kinases are directly coupled to the PIX family of nucleotide exchange factors, Mol. Cell 1 (1998) 183–192.

[28] S. Bagrodia, S.J. Taylor, K.A. Jordon, L. Van Aelst, R.A. Cerione, A novel regulator of p21-activated kinases, J. Biol. Chem. 273 (1998) 23633–23636.

[29] W.K. Oh, J.C. Yoo, D. Jo, Y.H. Song, M.G. Kim, D. Park, Cloning of a SH3 domain-containing proline-rich protein, p85SPR, and its localization in focal adhesion, Biochem. Biophys. Res. Commun. 235 (1997) 794–798.

[30] S.H. Park, Y.J. Im, S.H. Rho, J.H. Lee, S. Yang, E. Kim, S.H. Eom, Crystallization and preliminary X-ray crystallographic studies of the PDZ domain of shank1 from Rattus norvegicus, Acta Crystallogr. D 58 (2002) 1353–1355.

[31] Z. Otwinowski, W. Minor, Processing of X-ray diffraction data collected in oscillation mode, Methods Enzymol. 276 (1997) 307–326.

[32] A. Vagin, A. Teplyakov, MOLREP: an automated program for molecular replacement, J. Appl. Crystallogr. 30 (1997) 1022–1025.

[33] A.T. Brunger, P.D. Adams, G.M. Clore, W.L. DeLano, P. Gros, R.W. Grosse Kunstleve, J.-S. Jiang, J. Kuszewski, M. Nilges, N.S. Pannu, R.J. Read, L.M. Rice, T. Simonson, G.L. Warren, Crystallography & NMR system: a new software suite for macromolecular structure determination, Acta Crystallogr. D 54 (1998) 905–921.

[34] P. Emsley, K. Cowtan, Coot: model building tools for molecular graphics, Acta Crystallogr. D 60 (2004) 2126–2132.

[35] J.D. Thompson, T.J. Gibson, F. Plewniak, F. Jeanmougin, D.G. Higgins, The CLUSTAL_X windows interface: flexible strategies for multiple sequence alignment aided by quality analysis tools, Nucleic Acids Res. 25 (1997) 4876–4882.

[36] J.C. Phillips, R. Braun, W. Wang, J. Gumbart, E. Tajkhorshid, E. Villa, C. Chipot, R.D. Skeel, L. Kalé, K. Schulten, Scalable molecular dynamics with NAMD, J. Comput. Chem. 26 (2005) 1781–1802.

[37] W. Humphrey, A. Dalke, K. Schulten, "VMD - Visual Molecular Dynamics", J. Mol. Graphics 14 (1996) 33–38.

[38] R.A. Laskowski, M.W. MacArthur, D.S. Moss, J.M. Thornton, PROCHECK – A program to check the stereochemical quality of protein structures, J. Appl. Crystallogr. 26 (1993) 283–291.

[39] R.R. Penkert, H.M. DiVittorio, K.E. Prehoda, Internal recognition through PDZ domain plasticity in the Par-6–Pals1 complex, Nat. Struct. Mol. Biol. 11 (2004) 1122–1127.

[40] W.L. DeLano, The PyMOL Molecular Graphics System, DeLano Scientific, San Carlos, CA, 2002.